

*Paper presented at:  
Ocean Optics Conference XVI, 18-22 Nov. 2002, Santa Fe, USA*

## **ERROR PROPAGATION AT INVERSION OF IRRADIANCE REFLECTANCE SPECTRA IN CASE-2 WATERS**

*P. Gege  
German Aerospace Center (DLR), Remote Sensing Technology Institute,  
Oberpfaffenhofen, D-82234 Wessling, Germany  
[peter.gege@dlr.de](mailto:peter.gege@dlr.de)*

### **Abstract**

Many algorithms for determination of water constituents in case-2 waters make use of the Gordon approximation for the subsurface irradiance reflectance. It parameterises the water constituents by specific absorption and backscattering spectra. Based on specific optical properties of water constituents from Lake Constance, error propagation at inversion of the Gordon algorithm was investigated for concentration values typical for that lake. The following error sources were considered: proportionality factor  $f$  in the Gordon equation; curve forms of suspended matter backscattering spectra, Gelbstoff and phytoplankton absorption spectra; concentrations of phytoplankton, suspended matter and Gelbstoff; statistical noise; radiometric resolution. A ranking of the error sources is performed, required accuracies of model inputs are derived, and a strategy for finding suitable start values of the fit parameters is suggested.

### **Introduction**

Three groups of water constituents can be distinguished by remote sensing: phytoplankton, suspended matter, and Gelbstoff. Those waters where the concentrations of the three groups are weakly correlated or uncorrelated are called case-2 waters. In these waters the absorption and scattering properties of all three constituents have to be considered for quantitative determination of concentration from spectral measurements. This paper discusses how a wrongly determined concentration value of one water constituent influences the accuracy for the other constituents, and investigates errors induced by wrong model inputs and radiometric limitations of the sensor.

### **Irradiance reflectance model**

The subsurface irradiance reflectance spectrum  $R(\lambda)$  is expressed according to Gordon et al. (1975) as function of absorption  $a$  and backscattering  $b_b$  of the water body:

$$R(\lambda) = f \cdot \frac{b_b(\lambda)}{a(\lambda) + b_b(\lambda)}.$$

The factor of proportionality,  $f$ , depends on the scattering properties of the water and on the illumination and viewing geometry. There exist several algorithms to estimate or parameterise  $f$  (Aas 1987, Kirk 1991, Sathyendranath and Platt 1997). For clear sky conditions and high solar elevation  $f = 0.33$  is a good approximation (Gordon et al. 1975, Prieur 1976).

Backscattering  $b_b$  of the water body is calculated as the sum of backscattering by pure water and suspended particles:

$$b_b(\lambda) = b_{b,w}(\lambda) + X \cdot b_{b,X}^* \cdot (\lambda/\lambda_X)^n.$$

For pure water the empirical relation of Morel (1974) is used:

$$b_{b,w}(\lambda) = b_1 \cdot (\lambda/\lambda_1)^{-4.32}.$$

The factor of proportionality,  $b_1$ , depends on salinity. Here the fresh water value of  $b_1 = 0.00111 \text{ m}^{-1}$  for  $\lambda_1 = 500 \text{ nm}$  is taken. For oceanic water usually  $b_1 = 0.00144 \text{ m}^{-1}$  is set.

The backscattering of suspended matter is calculated as the product of concentration  $X$ , specific backscattering coefficient  $b_{b,X}^*$ , and a normalised scattering function  $(\lambda/\lambda_X)^n$ . The Angström exponent  $n$ , which determines the spectral shape, depends on particle size distribution. For large particles this parameter is near zero, for small particles it is typically in the order of  $-1$  (Sathyendranath et al. 1989).  $b_{b,X}^*$  is in the order of  $0.01 \text{ m}^2 \text{ g}^{-1}$  for  $\lambda_X = 500 \text{ nm}$  (Sathyendranath et al. 1989), but the values vary in lakes by more than one order of magnitude (Kutser et al. 2001). Here  $b_{b,X}^* = 0.0086 \text{ m}^2 \text{ g}^{-1}$  is set, which is a typical value for Lake Constance (Heege 2000).

The absorption of the water body is the sum of absorption of pure water and of all water constituents. Here the following parameterisation is used:

$$a(\lambda) = a_w(\lambda) + Y \cdot a_Y^*(\lambda) + C \cdot a_P^*(\lambda).$$

The pure water absorption spectrum  $a_w(\lambda)$  is taken from Buiteveld et al. (1994). Two groups of absorbing water constituents are considered: Gelbstoff (dissolved organic matter) and phytoplankton. Gelbstoff absorption is the product of concentration  $Y$  and specific absorption  $a_Y^*(\lambda)$ . For the spectrum  $a_Y^*(\lambda)$  the usual exponential approximation (Nyquist 1979, Bricaud et al. 1981) is taken:

$$a_Y^*(\lambda) = \exp[-S \cdot (\lambda - \lambda_0)].$$

Gelbstoff concentration  $Y$  is given in units of absorption at a reference wavelength  $\lambda_0$ . Here  $\lambda_0 = 440 \text{ nm}$  is chosen. The parameter  $S$  denotes the spectral slope.

The high number of phytoplankton species that occur in natural waters cause a wide natural variability of the absorption properties of phytoplankton. Here a spectrum  $a_P^*(\lambda)$  is used which is typical for Lake Constance (Heege 2000, Gege 2002). The phytoplankton concentration  $C$  is given as sum of chlorophyll-a and phaeophytin-a concentration.

In summary, the irradiance reflectance model uses 6 parameters ( $C$ ,  $X$ ,  $Y$ ,  $S$ ,  $n$ ,  $f$ ), 2 material constants ( $b_{b,X}^*$ ,  $b_1$ ) and 2 non-parametric spectra ( $a_w(\lambda)$ ,  $a_P^*(\lambda)$ ).

### Forward and inverse modeling

All simulations were done using the public domain software WASI = Water Colour Simulator (Gege 2002). 9 series of simulations have been performed for studying the influence of 9 error sources on the retrieval of  $C$ ,  $X$ ,  $Y$  from  $R(\lambda)$  spectra. Each series consists of a number of

forward calculations and corresponding inverse calculations of  $R(\lambda)$ . During forward modeling the parameter of interest was changed from a minimum value to a maximum value, while all other parameters were kept constant. During inversion the concentrations  $C$ ,  $X$ ,  $Y$  were fitted, while the parameter of interest was fixed at a certain value. The spectral range of all calculations was 400 to 900 nm, the spectral sampling interval was 1 nm.

The Simplex method (Nelder and Mead 1965) was taken as inversion algorithm. Minimisation of the residuals was done on the least squares of the linear reflectance values. (Least squares of the logarithmic reflectance values were also tested, but the results were much more sensitive to noise.) All wavelengths were weighted equally. It was verified that the results did not depend on the choice of the start values by performing most inversions twice: one time using the values of Table 1 as initial values, and one time using the "automatic determination of initial values" feature of WASI, which determines a "first guess" of  $C$ ,  $X$ ,  $Y$  from analytical equations (Gege 2002). The automatic method was not applied to noisy and dynamics-reduced spectra, because it failed when the spectrum was distorted significantly in the infrared.

A detailed explanation of the analysis is given at the example of  $S$  simulations (see Fig. 3); the other simulations are analogue. The simulations were performed for studying errors caused by the Gelbstoff absorption curve form, which is parameterised by  $S$ . In the forward mode a series of reflectance spectra was generated with different  $S$  values, while for the other parameters the values from Table 1 were used. This set was then inverted three times: first  $S$  was fixed at  $0.010 \text{ nm}^{-1}$ , then at  $0.014 \text{ nm}^{-1}$ , and finally at  $0.018 \text{ nm}^{-1}$ . During inversion  $C$ ,  $X$ ,  $Y$  were fitted, while all other parameters were kept constant. The result is shown in Fig. 3 left: the relative errors of  $C$ ,  $X$ ,  $Y$  are plotted as a function of the relative error of  $S$ . Each error curve consists of a coloured center curve, which is valid for a  $S$  value of  $0.014 \text{ nm}^{-1}$ , and a coloured band whose borders correspond to the lower and upper  $S$  values of  $0.010 \text{ nm}^{-1}$  and  $0.018 \text{ nm}^{-1}$ . Also shown (Fig. 3 right) is the forward modeled reflectance spectrum for the parameter values of Table 1 together with fit curves for two wrong  $S$  values, corresponding to relative errors of -25 % and +50 %. The appertaining errors of  $C$ ,  $X$ ,  $Y$  are listed in Table 1.

## Results

**Propagation of model parameter errors.** It was investigated which errors in the retrieved concentrations  $C$ ,  $X$ ,  $Y$  result from using wrong model inputs. In fact, the relative errors caused by wrong values of  $f$ ,  $n$  and  $S$ , and those from using a wrong spectrum  $a_p^*(\lambda)$ , were calculated. The results are shown in Figures 1 to 4:

- In case of  $f$ , the concentration errors don't depend on the value of  $f$ , only on its relative error. Wrong  $f$  factors affect mainly  $X$ . Errors for  $C$  are small and errors for  $Y$  negligible.
- $n$  is typically in the range of 0 to -1, thus  $n$  errors are in most cases below  $\pm 1$  (absolute). These cause  $Y$  errors up to ~50 % and  $C$ ,  $X$  errors below 30 %.  $C$  errors increase at low  $n$  values.
- An important error source is  $S$ : Wrong  $S$  values cause very large errors for  $C$  (easily above 100 %), large errors for  $Y$ , but almost no errors for  $X$ .
- Errors caused by wrong spectra  $a_p^*(\lambda)$  are difficult to quantify since  $a_p^*(\lambda)$  is not parameterised. Here 5 spectra were used which have been shown to characterise the phytoplankton in Lake Constance from a remote sensing point of view (Gege 1998). The large errors in  $C$  retrieval suggest to rescale the 5 spectra. Errors for  $X$  and  $Y$  are relatively small.

**Propagation of concentration errors.** It was investigated how a wrongly determined concentration value of one water constituent influences the accuracy for the other constituents. The results are shown in Figures 5, 6, 7:

- Errors of C cause only minor errors for the other water constituents, except errors at high C cause high Y errors.
- Errors of X cause very large errors in C (easily above 100 %) and large errors of Y.
- Errors of Y cause very large errors in C (easily above 100 %), but have almost no influence on X.

**Propagation of sensor limitations.** It was investigated which errors in the retrieved concentrations C, X, Y result when the spectrum  $R(\lambda)$  is deteriorated by sensor noise or insufficient radiometric dynamics. The results are shown in Figures 8 and 9: Both sensor properties affect mainly the accuracy of C (statistical errors in the order of 10-20 %), while the accuracies of X and Y are little impaired. It should be noted, however, that a high number of spectral channels compensates radiometric sensor deficiencies to some extent; the results will be very different for sensors with less channels.

**Error ranking.** A comparison of the 9 error sources is given in Table 1. For each parameter the resulting errors of C, X, Y are listed at two wrong parameter values. Based on this table, a ranking of the errors is made in Table 2. It comprises all error sources which cause errors above  $\pm 25\%$  in Table 1.

Par.	Value	Par. error	C error	X error	Y error	Par. error	C error	X error	Y error
f	0.4	-25%	17%	36%	1%	50%	10%	-35%	3%
n	0	-0.5	-17%	14%	26%	0.5	12%	-12%	-22%
S	$0.014 \text{ nm}^{-1}$	-25%	158%	3%	-31%	50%	193%	7%	-35%
$a_p^*(\lambda)$	spectrum	mean	56%	3%	9%	max	-100%	-8%	-21%
C	$2 \mu\text{g l}^{-1}$	-25%	—	-3%	7%	50%	—	5%	-10%
X	$2 \text{ mg l}^{-1}$	-25%	-100%	—	-9%	50%	376%	—	-38%
Y	$0.3 \text{ m}^{-1}$	-25%	49%	4%	—	50%	-100%	5%	—
noise	StdDev	0.001	$\pm 10\%$	$\pm 1\%$	$\pm 3\%$	0.002	$\pm 20\%$	$\pm 2\%$	$\pm 5\%$
dynamics	$\Delta R$	0.001	$\pm 5\%$	0	$\pm 1\%$	0.002	$\pm 10\%$	$\pm 1\%$	$\pm 2\%$

**Table 1: Comparison of errors.**

Rank	C		X		Y	
1	X	$\pm 3.4\%$	f	$\pm 19\%$	S	$\pm 20\%$
2	S	$\pm 3.5\%$	—	—	X	$\pm 33\%$
3	Y	$\pm 6.5\%$	—	—	n	$\pm 0.48$
4	$a_p^*(\lambda)$	$\pm 25\%$	—	—	—	—

**Table 2: Ranking of error sources and required accuracies for concentration errors below  $\pm 25\%$ .**

**Required accuracies.** As a result of the simulations, more and less critical error sources for the retrieval of water constituents have been identified. Table 2 provides a ranking of the critical error sources, and it lists the accuracies required to obtain concentration errors below 25 % from a single error source. The resulting sensitivity to errors is very different for the retrieval of chlorophyll, suspended matter and Gelbstoff:

- Highly sensitive to errors is the determination of phytoplankton concentration: 3 parameters must be known very accurately to avoid large errors. The main error source is Gelbstoff, which contributes 2 critical parameters: spectral shape and concentration. Both parameters must be known with an accuracy of few percent. The second important error source is suspended matter, where also few percent concentration error is critical. The third error source,  $a_p^*(\lambda)$ , represents a conversion factor from "optical" to gravimetric phytoplankton concentrations, which is highly variable in nature.
- Quite robust is the retrieval of suspended matter: the only notable error source is the  $f$  factor, which can be determined, however, with little error from models. The main problem for suspended matter is the conversion from "optical" to gravimetric concentrations, since the conversion factor  $b_{b,X}^*$  is highly variable in nature.
- The accuracy of Gelbstoff retrieval is not critically affected by errors. Main error source is the spectral shape of the Gelbstoff absorption spectrum. For the other error source, suspended matter, relatively large errors concerning concentration and spectral shape of backscattering are acceptable.

## Conclusions

Summarising the results, the determination of "optical" concentrations from irradiance reflectance spectra by inversion is very differently sensitive to errors for the different water constituents: the sensitivity is very small for suspended matter, small for Gelbstoff, but very high for phytoplankton. The conversion from "optical" to gravimetric concentrations is an additional error source; this subject was only touched at the example of phytoplankton.

The results can be applied to the initial values problem of inversion. It is the problem that the inversion algorithm may not find the correct values of the fit parameters if the start values are too different from the correct values. Correct are those values for which the correspondence between fit curve and given spectrum is maximal. The problem is caused by the fact that different sets of model parameters yield similar reflectance spectra. For illustration sample fit curves are shown for each simulation, see the right diagrams of all Figures. In many cases the fit curve is very close to the forward modeled spectrum, although one parameter is significantly wrong. Thus, if inversion is started using a set of parameter values which correspond to a curve that is already similar to the given spectrum, the correct set of fit parameters may not be found. This can happen in particular if the spectrum is deteriorated by noise or calibration errors, or if spectral features are present which are not included in the model, e.g. absorption of detritus and inorganic particles or fluorescence of Gelbstoff and phytoplankton.

Based on Table 2, a two-steps procedure is suggested for determining initial values:

- The first step determines an accurate start value of  $X$  and a "first guess" of  $Y$ . Fit parameters are  $X$  and  $Y$ , all other parameters are kept constant. The result for  $X$  is quite accurate since  $X$  is very little affected by errors. The result for  $Y$  depends mainly on the accuracy of the start values of  $S$  and  $n$ .
- The second step determines a start value of  $C$  and suited start values of  $Y$  and  $S$ . Fit parameters are  $C$ ,  $Y$  and  $S$ . The strategy is to fit simultaneously with  $C$  all parameters which cause large errors for  $C$  determination. These are  $Y$  and  $S$ , while  $X$  is known accurately from the first step.

The limitations of this procedure need further investigations.

## References

- E. Aas (1987): Two-stream irradiance model for deep waters. *Applied Optics* 26(11), 2095-2101.
- A. Bricaud, A. Morel, L. Prieur (1981): Absorption by dissolved organic matter of the sea (yellow substance) in the UV and visible domains. *Limnol. Oceanogr.* 26, 43-53.
- H. Buiteveld, J. H. M. Hakvoort, M. Donze (1994): The optical properties of pure water. *SPIE Vol. 2258, Ocean Optics XII*, 174-183.
- P. Gege (1998): Characterization of the phytoplankton in Lake Constance for classification by remote sensing. *Arch. Hydrobiol. Spec. Issues Advanc. Limnol.* 53, p. 179-193.
- P. Gege (2002): The Water Colour Simulator WASI. User manual for version 2. *DLR Internal Report IB 564-01/02*, 60 p. (Download of report and software from the ftp server ftp.dfd.dlr.de, directory /pub/WASI, anonymous login with email-address as password.)
- H. R. Gordon, O. B. Brown, M. M. Jacobs (1975): Computed Relationships between the Inherent and Apparent Optical Properties of a Flat Homogeneous Ocean. *Applied Optics* 14, 417-427.
- T. Heege (2000): Flugzeuggestützte Fernerkundung von Wasserinhaltsstoffen im Bodensee. *PhD thesis. DLR-Forschungsbericht 2000-40*, 141 p.
- J. T. O. Kirk (1991): Volumen scattering function, average cosines, and underwater lightfield. *Limnol. Oceanogr.* 36, 455-467.
- T. Kutser, A. Herlevi, K. Kallio, H. Arst (2001): A hyperspectral model for interpretation of passive optical remote sensing data from turbid lakes. *The Science of the Total Environment* 268 (2001), 47-58.
- A. Morel (1974): Optical Properties of Pure Water and Pure Sea Water. In: N. G. Jerlov, E. Steemann Nielsen (Eds.): *Optical Aspects of Oceanography*. Academic Press London, 1-24.
- J. A. Nelder, R. Mead (1965): A simplex method for function minimization. *Computer Journal* 7, 308-313.
- G. Nyquist (1979): Investigation of some optical properties of seawater with special reference to lignin sulfonates and humic substances. *PhD Thesis, Göteborgs Universitet*, 200 p.
- L. Prieur (1976): Transfers radiatifs dans les eaux de mer. *Thesis, Doctorat d'Etat, Univ. Pierre et Marie Curie, Paris*, 243 pp.
- S. Sathyendranath, L. Prieur, A. Morel (1989): A three-component model of ocean colour and its application to remote sensing of phytoplankton pigments in coastal waters. *Int. J. Remote Sensing* 10, 1373-1394.
- S. Sathyendranath, T. Platt (1997): Analytic model of ocean color. *Applied Optics* 36, 2620-2629.

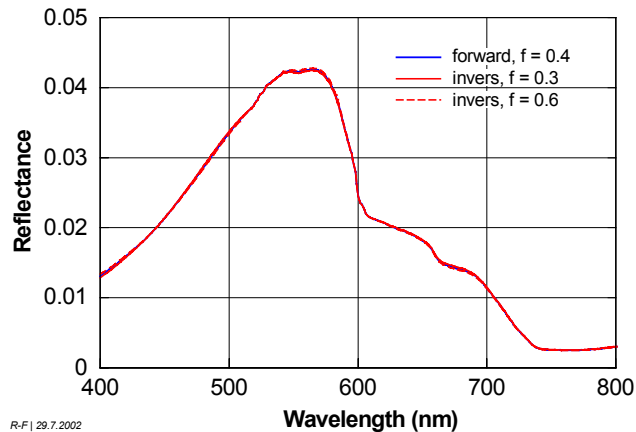
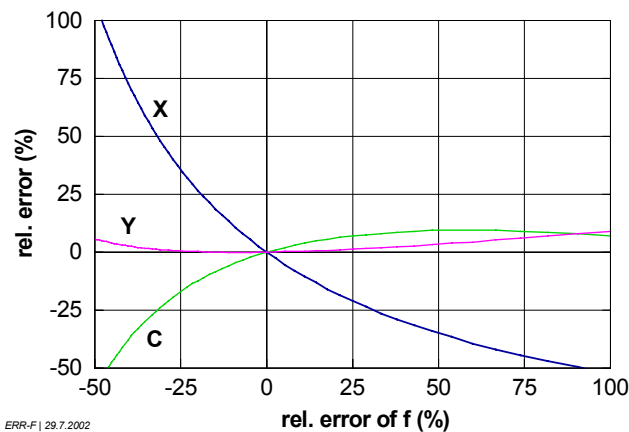


**Fig. 1: Propagation of  $f$  errors. Left: Errors for C, X, Y retrieval for  $f = 0.3, 0.4, 0.5$  (identical results). Right: Best fit curves for wrong  $f$  values.**

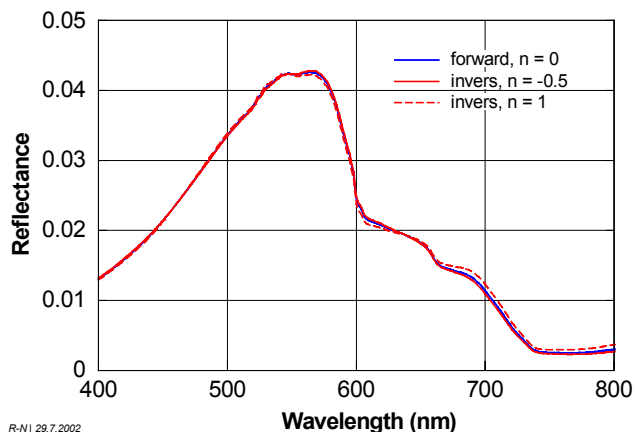
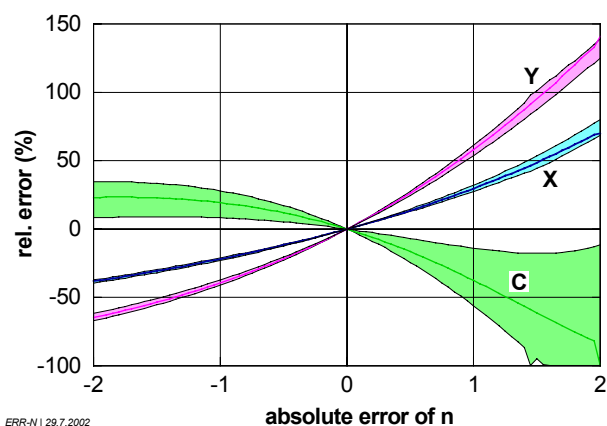


**Fig. 2: Propagation of  $n$  errors. Left: Errors for C, X, Y retrieval for  $n = 0$  (coloured lines),  $-1$  and  $1$  (borders of shaded areas). Right: Best fit curves for wrong  $n$  values.**

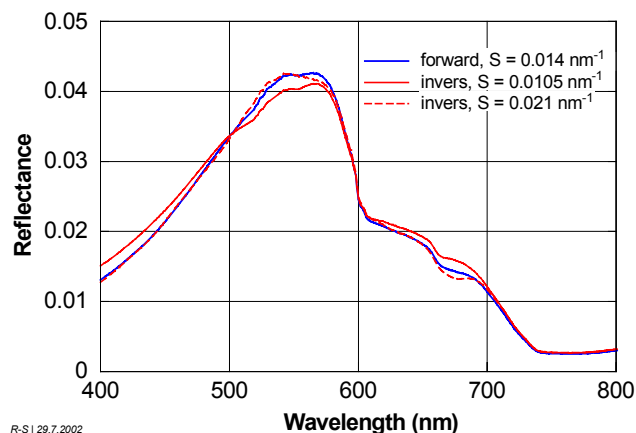
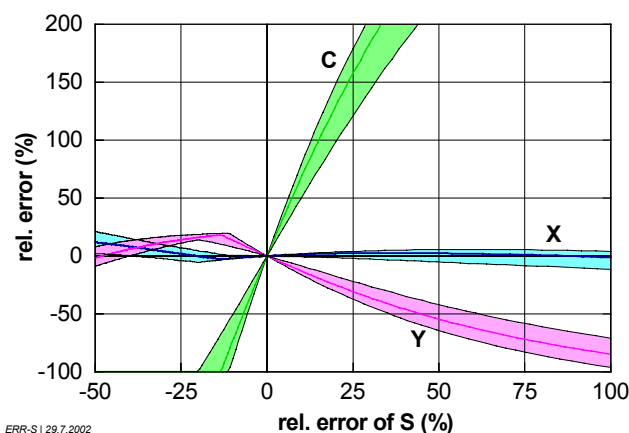
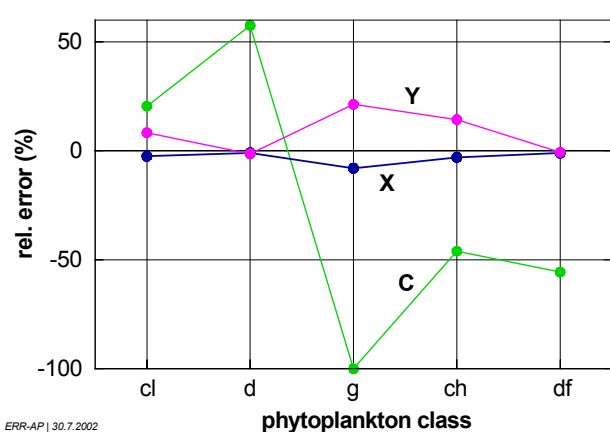
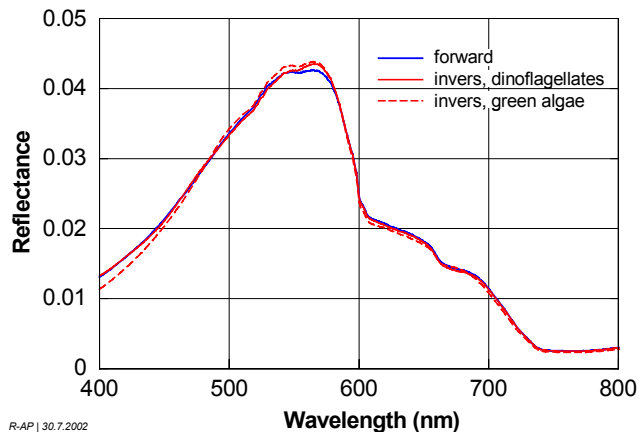


**Fig. 3: Propagation of  $S$  errors. Left: Errors for C, X, Y retrieval for  $S = 0.014$  (coloured lines),  $0.010$  and  $0.018 \text{ nm}^{-1}$  (borders of shaded areas). Right: Best fit curves for wrong  $S$  values.**

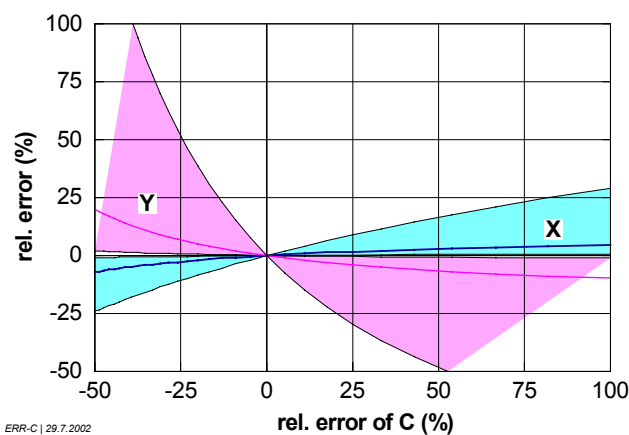


ERR-AP | 30.7.2002

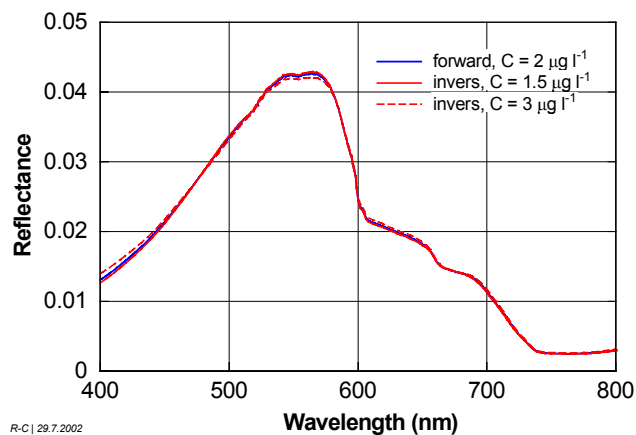


R-AP | 30.7.2002

**Fig. 4: Influence of spectrum  $a_p^*(\lambda)$  on C, X, Y retrieval.** During inversion  $a_p^*(\lambda)$  has been exchanged successively by absorption spectra of two cryptophyta species with low (cl) and high (ch) phycoerythrin concentration, diatoms (d), green algae (g) and dinoflagellates (df). Left: Errors for C, X, Y retrieval. Right: Best fit curves for wrong phytoplankton absorption spectra.

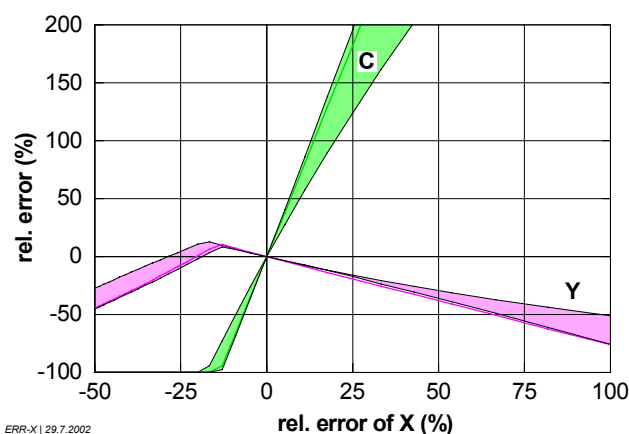


ERR-C | 29.7.2002

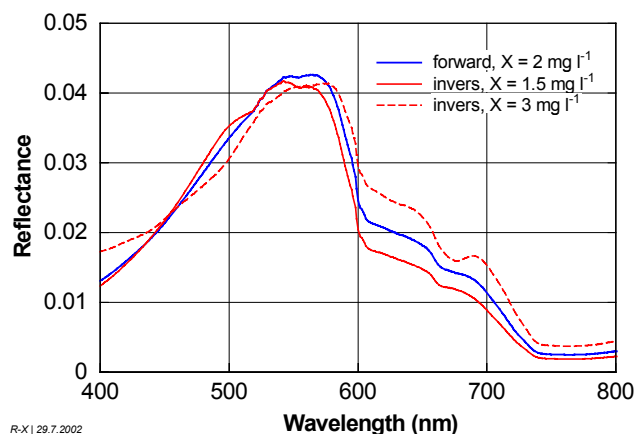


R-C | 29.7.2002

**Fig. 5: Propagation of C errors.** Left: Errors for X, Y retrieval for C = 2 (coloured lines), 0.2 and 20  $\mu\text{g l}^{-1}$  (borders of shaded areas). Right: Best fit curves for wrong C values.



ERR-X | 29.7.2002



R-X | 29.7.2002

**Fig. 6: Propagation of X errors.** Left: Errors for C, Y retrieval for X = 2 (coloured lines), 0.2 and 20  $\text{mg l}^{-1}$  (borders of shaded areas). Right: Best fit curves for wrong X values.



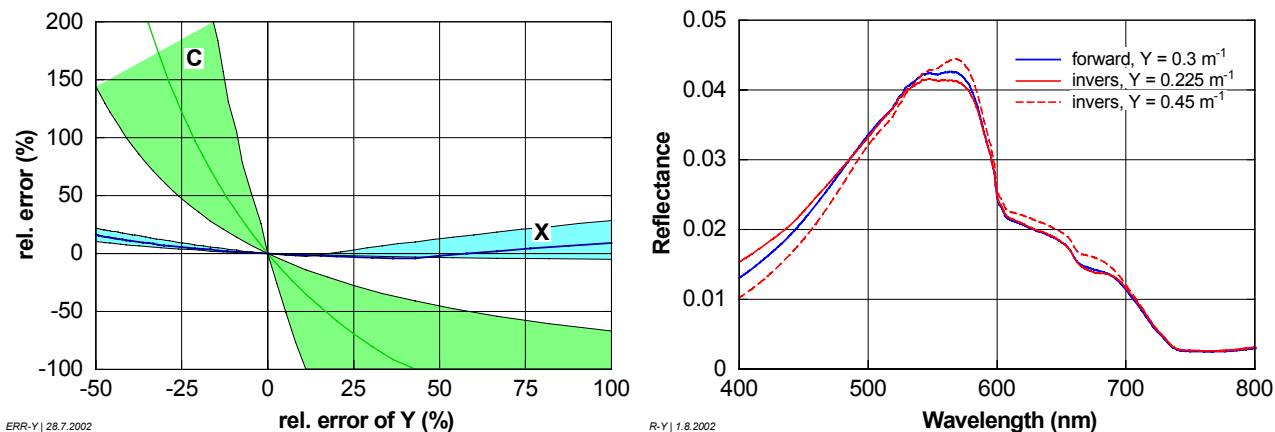


Fig. 7: Propagation of Y errors. Left: Errors for C, X retrieval for  $Y = 0.3$  (coloured lines), 0.1 and  $1 \text{ m}^{-1}$  (borders of shaded areas). Right: Best fit curves for wrong Y values.

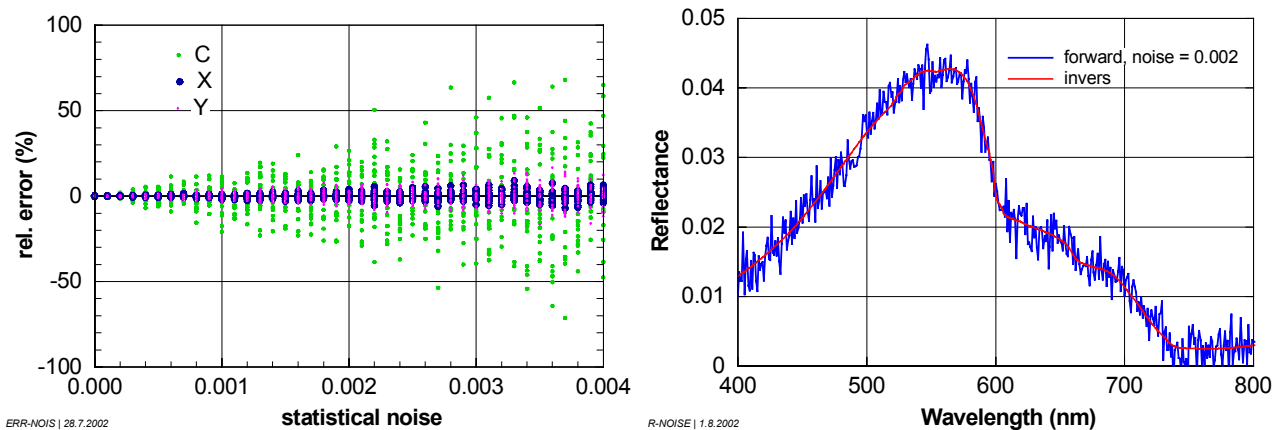


Fig. 8: Propagation of statistical noise. Left: Errors for C, X, Y retrieval. At each noise level 20 spectra were calculated and inverted. Right: Best fit of a reflectance spectrum with noise of 0.002.

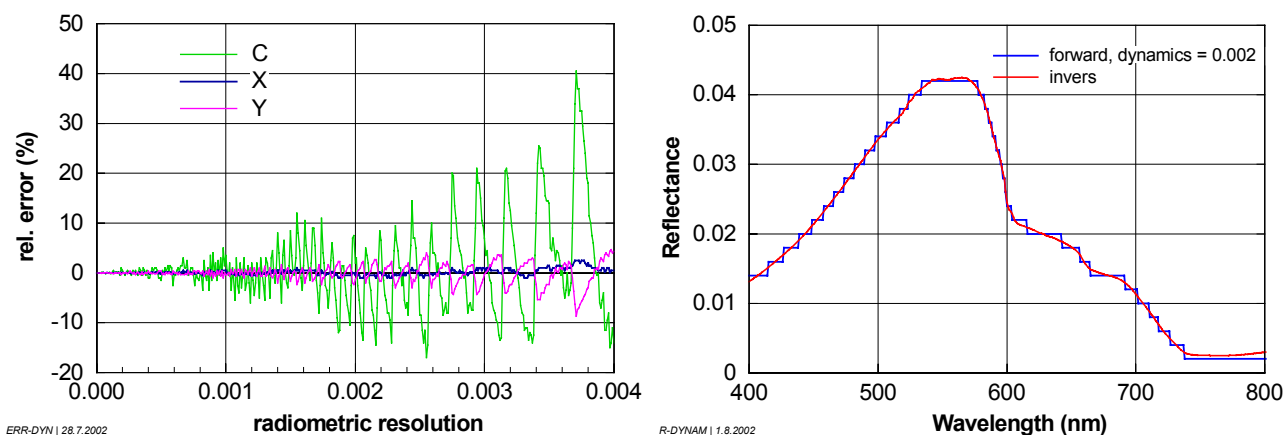


Fig. 9: Propagation of radiometric dynamics. Left: Errors for C, X, Y retrieval. Right: Best fit of a reflectance spectrum with a dynamics of 0.002.